A&A manuscript no.
(will be inserted by hand later)

Your thesaurus codes are:
03(11.17.1;11.17.4;02.16.2)

ASTRONOMY AND ASTROPHYSICS
February 29, 2000

Spectropolarimetry of the iron low ionization broad absorption line quasar Q 0059-2735*

H. Lamy and D. Hutsemékers **, ***

Institut d'Astrophysique et de Géophysique, Université de Liège, 5, Avenue de Cointe, B-4000 Liège, Belgium

Received date; accepted date

Abstract. We present optical (ultraviolet rest-frame) spectropolarimetric observations of the rare iron low ionization broad absorption line (BAL) QSO Q 0059-2735. The continuum polarization increases to the blue with a regular rotation of the polarization position angle, suggesting that at least two mechanisms are at the origin of the polarization. There is also some evidence for dilution by a Fe II pseudo-continuum in emission. In the broad absorption lines, the polarization strongly rises, with the largest values ever reported. On the contrary, the Fe II blends in absorption are not more polarized than the continuum, while they are clearly visible in the polarized flux. These different polarization properties of Fe II absorption lines suggest a different origin and/or geometry. The observed properties of Q 0059-2735 are consistent with a hybrid QSO / starburst model.

Key words: Quasars : absorption lines - Quasars : individual : Q 0059-2735 - Polarization

1. Introduction

Broad absorption line (BAL) QSOs are a class of QSOs with broad, often deep, absorption troughs of high-ionization species like C IV, Si IV or N V, blueshifted with respect to the corresponding emission lines. These BALs are observed in $\sim 12\,\%$ of optically selected QSOs and are generally interpreted in terms of material outflowing at very high velocities ($\sim 0.1c$). Since the emission lines and continuum properties of BAL and non-BAL QSOs appear essentially similar (Weymann et al 1991), all radio-quiet (RQ) QSOs may have a broad absorption region of small covering factor, the QSOs being classified as BAL QSOs when the line-of-sight intercepts absorbing material. On the other hand, the BAL QSOs may form a different class of objects with large covering factor, possibly in an early stage of an evolutionary process towards normal QSOs (e.g. Boroson & Meyers 1992).

Among the BAL QSOs, $\sim 15\,\%$ constitute a sub-class with additional low-ionization broad absorption troughs : the low-ionization (LI) BAL QSOs. These QSOs generally have redder continua, stronger optical Fe II emission and very weak [O III] emission while detectable. These properties are consistent with LIBAL QSOs being more dusty (Boroson & Meyers 1992, Sprayberry & Foltz 1992).

Q 0059-2735 (z = 1.59) is a peculiar member of the LIBAL QSO class. First, the large Balmer decrement and the optical / near-infrared color index indicate an unusually high amount of dust in its surroundings (Egami et al. 1996). Also, the emission lines from highly ionized species are particularly weak and narrow (Hazard et al. 1987). But, most striking, is the fact that its rest-frame ultraviolet spectrum contains many narrow absorption lines (NAL) from highly-excited metastable levels of iron-peak elements, which sometimes blend in broad troughs, then forming a complex absorption spectrum (Hazard et al. 1987, Wampler et al. 1995). Up to now only three other QSOs are known to show similar properties, forming the class of *iron* LIBAL QSOs, of which Q 0059-2735 is often considered as the prototype (Becker et al. 1997, Brotherton et al. 1997). Detailed analysis of high-resolution spectra suggests that Fe II absorption may originate from low ionization condensations embedded in a hotter BAL flow (Wampler et al. 1995). An alternative model is that Q 0059-2735 is a mixture of a QSO and a starburst galaxy (Cowie et al. 1994, Egami et al. 1996). In this view, the Fe II absorption could be related to gas swept up by supernova explosions in the starburst galaxy.

Like several other LIBAL QSOs, Q 0059-2735 is significantly polarized in the continuum (Hutsemékers et al. 1998), providing us with the possibility of carrying out a detailed spectropolarimetric study. Such observations are presented here with the aim of better understanding the geometry of this object as well as the origin of the Fe II absorption lines.

2. Observations and data reduction

The observations were carried out with the ESO 3.6m telescope at the European Southern Observatory (La Silla, Chile) on September 10-12, 1996. The telescope was equipped with EFOSC1 and a Wollaston prism, giving two orthogonally polarized bi-dimensional spectra of the object and of the sky,

* Based on observations collected at the European Southern Observatory, La Silla, Chile

** Also, Chercheur Qualifié au Fonds National de la Recherche Scientifique (FNRS, Belgium)

*** Present address : ESO, Casilla 19001, Santiago, Chile separated by 20" on the CCD detector. The detector was a 512×512 TeK CCD (ESO#26) with a pixel size of 27 μm corresponding to 0.″605 on the sky (Melnick et al. 1989). Two exposures with the Wollaston prism rotated by 45° were secured to obtain the two Stokes parameters fully describing the linear state of polarization. A mask was used in order to avoid overlapping of the sky spectra. The spectrum covers the useful 3700–8700 Å spectral range after combining the B300 and R300 grisms. The spectral resolution is 6.3 Å per pixel. For each grism and position angle of the Wollaston, three frames were taken for a total exposure time of 90 minutes.

All reductions were performed using procedures developed within the ESO MIDAS software package. After the usual bias and flat-field corrections, one-dimensionnal spectra were carefully extracted and calibrated in wavelength and flux, independently for the ordinary and extraordinary spectra. The standard star EG274 (Stone & Baldwin 1983, Baldwin & Stone, 1984), assumed to be unpolarized, was observed with the same setup and used for the flux calibration and for an estimate of the instrumental polarization. For each of the two spectra of the object, the sky was averaged using the nearest adjacent strips of same polarization on either side of the object. These sky spectra were then individually extracted and calibrated before subtraction from the object spectra. The one-dimensional spectra were rebinned on a linear wavelength scale with 13 Å pixels, (approximately corresponding to 2 original pixels) in order to increase the signal-to-noise ratio while keeping a good spectral resolution. Finally, these spectra were combined with the usual formulae to derive the q and u normalized Stokes parameters. (cf. di Serego Alighieri 1998). The associated errors were calculated by propagating the errors from the photon noise in the object and sky spectra. Note the instrumental polarization measured from EG274 was found to be low ($\sim 0.3\,\%$). A spectropolarimetric standard star, HD161291, was observed with the same setup in order to fix the zero point of the polarization position angle (PA) and to check the whole procedure. The interstellar polarization curve of HD161291 was found to be in excellent agreement with that measured by di Serego Alighieri et al. (1994) with the same setup, and with the parameters given by Serkowski et al. (1975)

Note that other BALQSOs were observed at the same time and compared to spectropolarimetric data available in the literature (Cohen et al. 1995, Goodrich & Miller 1995, Schmidt & Hines 1999). Our results appear in good agreement, giving additional confidence in the observation / reduction process. More details about these observations will be given elsewhere.

3. Results

3.1. Analysis of data

The optical (UV rest-frame) spectropolarimetric results for Q 0059-2735 are displayed in Fig. 1. The polarization degree p, the polarization position angle θ and the associated uncertainties σ_p and σ_θ have been computed from the q and u normalized Stokes parameters using the usual formulae (e.g. di

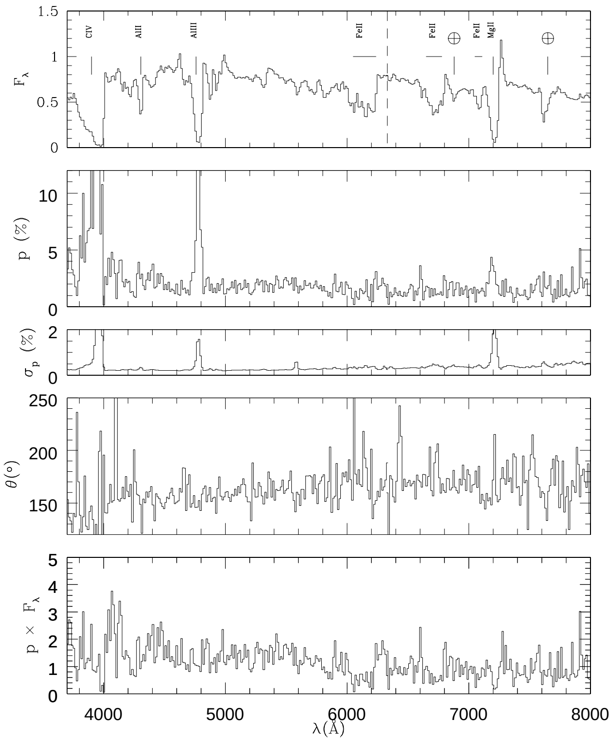

Fig. 1. Spectropolarimetry of Q0059-2735. From top to bottom : (1) The total flux, F_λ, in arbitrary units (2) The degree of polarization, p (3) The uncertainty on the degree of polarization, σ_p (4) The polarization position angle, θ (5) The polarized flux, $p\ \times\ F_\lambda$ in arbitrary units. The B300 and R300 spectra were cut on their reddest and bluest parts respectively, and linked together at the wavelength indicated by the vertical dashed line. The less interesting part above 8000 Å is not shown here. Note finally that p in C IV and Al III, and σ_p in C IV are truncated; peak values are given in Table 2

Serego Alighieri 1998). The combined B300 and R300 spectra are presented.

Moreover, the continuum polarization has been measured from the Stokes q, u spectra in wavelength bands selected after a careful inspection of the high-resolution spectra of Wampler et al (1995) in order to avoid the numerous Fe II narrow absorption lines. The continuum defined in that way is the sum of the QSO continuum and of the possible pseudo-continuum formed by the Fe II emission. The measurements are reported in Table 1. The continuum polarization of Q 0059-2735 slightly decreases towards the red (from 2% to 1%). These values are in good agreement with our previous broad-band polarimetry measurements: $p_V = 1.62 \pm 0.29\,\%$ and $1.45 \pm 0.23\,\%$ (Hutsemékers et al 1998, Lamy & Hutsemékers 2000). However, at the red end of the spectrum, the polarization starts rising again. This is confirmed by the value measured in the Gunn i filter during the same run ($p_i = 2.45 \pm 0.24\,\%$, Lamy & Hutsemékers 2000). The polarization position angle slightly rotates along the blue part of the spectrum. This rotation could indicate the presence of two polarization mechanisms, or the sum of two polarized components coming from distinct regions. Indeed, in this latter case, if the relative importance of one component com-

Table 1. Continuum polarization

	$\overline{p}$	$\overline{\sigma_p}$	$\overline{\theta}$	$\overline{\sigma_\theta}$
$\lambda\lambda\, 4400 - 4600$	1.98	0.05	152	1
$\lambda\lambda\, 5000 - 5200$	1.70	0.06	160	1
$\lambda\lambda\, 5600 - 5800$	1.67	0.07	166	2
$\lambda\lambda\, 6250 - 6400$	1.52	0.08	170	2
$\lambda\lambda\, 7350 - 7500$	0.85	0.10	169	4
$\lambda\lambda\, 7750 - 8000$	1.57	0.12	166	3

Table 2. BAL trough polarization

	$\overline{p}$	$\overline{\sigma_p}$	p_{peak}	$\sigma_{p_{peak}}$
C IV $\lambda\, 1549$	8.99	0.16	48.0	3.32
Al II $\lambda\, 1671$	2.65	0.18	3.92	0.34
Al III $\lambda\, 1857$	7.32	0.25	17.2	1.60
Mg II $\lambda\, 2798$	2.14	0.46	4.36	0.94
Fe II $\lambda\, 2380$	0.97	0.09	2.45	0.38
Fe II $\lambda\, 2600$	1.20	0.12	2.74	0.32
Fe II $\lambda\, 2750$	1.11	0.18	1.64	0.34

pared to the other one changes with wavelength, one also expects a rotation of the polarization PA. Again, in the red part of the spectra, this rotation stops and the value of θ measured in the Gunn i filter ($\theta_i = 166 \pm 3\,\%$) is close to the one measured redward of Mg II.

We have also measured the polarization in the BAL troughs. Peak and integrated values are given in Table 2. To calculate the integrated values, we assumed a power-law for the continuum using the spectral indices ($\alpha_B = 1.50$ and $\alpha_R = 1.59$) measured in Hutsemékers et al. (1998) and we defined the broad absorption lines as those regions of the spectra dipping 10% or more below the estimated continuum, thus following the prescriptions of Weymann et al (1991) for C IV. Then the q and u spectra were averaged over the BALs and combined to obtain the $\overline{p}$ values given in Table 2. As previously observed in many other BAL QSOs (Goodrich & Miller 1995, Ogle 1997, Schmidt & Hines 1999), the degree of polarization strongly increases in the BAL troughs. However, in Q 0059-2735, the peak values reached in the C IV and Al III BALs are unusually high (respectively 48 % and 17 % measured on the spectrum rebinned to 13 Å), larger than observed in any other BAL QSO (Schmidt & Hines 1999). Note that these are not spurious results since adjacent pixels have also high values. They may even be lower limits since we do not resolve the peak. These large values preclude resonance scattering in the BAL lines as the main polarizing mechanism (Lee et al. 1994). The LI BALs Al II and Mg II are also polarized but at a lower level above the continuum. It is interesting to remark that the polarization peak in Mg II seems to correspond to the higher velocity part of the BAL. A possible rotation of θ across C IV and Mg II may be present but the signal-to-noise ratio is too low to distinguish from the regular rotation accross the continuum. In the polarized flux, while the BAL C IV and Mg II appear quite clearly, there is no indication of the presence of the BAL Al III, even in the non-rebinned data.

Also remarkable is the different behavior of the Fe II absorption blends which, contrary to what happens in other BALs, show no significant polarization increase in the absorption troughs (Table 2), although the degree of polarization varies across the blends in a complicated way. However, some of these blends appear in the polarized flux, clearly for Fe II $\lambda\, 2380$ and Fe II $\lambda\, 2600$, and marginally for Fe II $\lambda\, 2750$. A few other NALs may also be visible in the polarized flux (e.g. Ni II or Zn II) but higher S/N data should be obtained to confirm them.

Finally, the polarization of the Mg II emission line appears similar to that of the continuum. On the other hand, while no C IV broad emission is seen in the direct flux, a broad emission seems present in the polarization spectrum and more particularly in the polarized flux.

3.2. Comparison with similar objects

A few other QSOs also exhibit narrow absorption lines from metastable levels of iron FIRST J 0840+3633 and J 1556+3517, Becker et al. 1997; Hawaii 167, Cowie et al. 1994), and spectropolarimetric data have been obtained for two of them (J 0840+3633 and J 1556+3517, Brotherton et al. 1997).

J 0840+3633 has essentially the same spectral features as Q 0059-2735 albeit with deeper absorption troughs (Becker et al. 1997). The polarization significantly increases in the LI BALs Al III and Mg II although not as much as for Q 0059-2735 (peak values around 8 %). It rises weakly in the Fe II blends at 2600 Å and 2750 Å and drops in Fe II 2380 Å (Brotherton et al. 1997). The polarization PA rotates accross these Fe II blends in a complex manner. All these lines including the Al III BAL are strongly apparent in the polarized flux.

J 1556+3517 has a much more heavily absorbed and reddened continuum and no prominent emission lines (Becker et al. 1997). It also has polarimetric characteristics completely different from other BAL QSOs. The degree of polarization in the continuum is high (p = 7 % around 7000 Å) and rises strongly to the blue (p = 13 % around 5000 Å). Moreover, it dramatically *decreases* to zero in the broad absorption lines (including in the Fe II blends), indicating that the scattered flux is completely absorbed at these wavelengths (Brotherton et al. 1997). The polarization PA rotates accross the broad absorption lines and the Fe II blends.

4. Discussion and conclusions

Since the continuum polarization slightly rises towards the blue and since the QSO is redder than typical radio-quiet QSOs, the polarization may be attributed to dust scattering. However, a wavelength-independent scattering by free electrons is also possible if a dilution by an unpolarized red component is present. The latter may be due to a wavelength-dependent extinction stronger for the direct rays than for the scattered ones, or to the pseudo-continuum formed by the blends of numerous unpolarized Fe II narrow emission lines, as suggested for J 0840+3633 and PHL 5200 (Brotherton et al. 1997, Cohen et al. 1995, Wills et al. 1985). If true, we would expect a rise of polarization redward of Mg II, where optical Fe II lines are much weaker ($\lambda \geq 7750$ Å, Wills et al. 1985). And indeed, although the quality of the measurements is poorer in this region, the values in Table 1 as well as our Gunn i measurement confirm this rise at the red end of our spectra. However, the still higher p at the blue end of the spectrum and the regular rotation of the polarization PA cannot be explained by the Fe II dilution alone. It is therefore likely that at least one other mechanism acts simultaneously, dust scattering and/or differential extinction. Note that dust scattering of the C IV broad emission line photons in the vicinity of the broad absorption line region (BALR) could explain their destruction in the direct flux and their presence in the polarized flux.

In agreement with the standard interpretation of BAL QSO spectropolarimetry (Cohen et al. 1995, Schmidt & Hines 1999), the rise of polarization in the BAL troughs suggests that the scattered continuum is less absorbed in the BALR than the direct unpolarized continuum. Furthermore, the fact that some BALs (e.g. C IV) are seen in the polarized flux indicates that the scattered flux crosses the BALR in regions of lower opacity. However, the absence of Al III in the polarized flux suggests that the scattered flux misses the region of the BALR where Al III is formed. This behavior is not unique among BAL QSOs: in the polarized flux of Q 1246-0542 there is apparently no trace of any BAL, including C IV (Schmidt & Hines 1999[1]). In the case of Q 0059-2735, this suggests that the low-ionization Al III BALR is less extended than the high-ionization one, and does not cover the scattering region. On the contrary, the Fe II absorption blends are detected in the polarized flux, while they are not significantly more polarized than the continuum. Thus, the iron absorbing gas must intercept both the polarized and unpolarized continua with roughly the same opacity, suggesting a different location and/or geometry for the Fe II absorbing region. Compared to other low-ionization BALs, the behavior of the Mg II BAL is quite striking since it appears more polarized than the continuum (although not as much as Al III), while it is seen in the polarized flux like Fe II. These intermediate properties may indicate a hybrid origin for the Mg II BAL.

Our results are consistent with the interpretation that the spectrum of Q 0059-2735 is a superposition of a BAL QSO spectrum and of a starburst one, the starburst being at the origin of the Fe II NALs and of the unusually large reddening (cf. Cowie et al. 1994; Egami et al. 1996). In this model, Q 0059-2735 is seen along a line of sight close to the dusty equatorial plane. In the framework of the disk-wind model for the QSO BALR, such an orientation could explain the presence of low ionization troughs, the very deep and steep CIV absorption trough, and the high degree of polarization in the continuum (cf. Murray et al. 1995, Hutsemékers et al. 1998). Free electrons and/or dust scatter the continuum photons along lines of sight that cross parts of the BALR where the opacity is still large for C IV, and much smaller for Al III and Mg II, the latter ones originating much closer to the disk as suggested by Murray et al. (1995).

Within this model, the Fe II absorption blends are produced beyond the BALR, in material swept up by the strong winds of supernovae in the starburst (Hazard et al. 1987, Norman et al. 1994). The BAL Mg II could be hybrid, partly formed in the QSO disk-wind and partly in the starburst. The fact that the Mg II polarization peak does not exactly correspond to the BAL peak could support this hypothesis, although data with higher spectral resolution are needed to confirm it.

Since J 0840+3633 has basically the same properties as Q 0059-2735, this QSO + starburst model may apply as well, assuming that the scattered flux now crosses the low-ionization BALR (Al III is detected in the polarized flux). The smaller peak values of the BAL polarization in J 0840+3633 are compatible with this hypothesis, the scattered flux crossing regions of higher opacity than in Q 0059-2735.

Acknowledgements. This research is supported in part by the contracts ARC 94/99-178, and by PAI P4/05.

[1] Note that we confirm the absence of BAL in the polarized flux of Q1246-0542 on the basis of new data obtained with a better signal-to-noise ratio (Lamy & Hutsemékers 2000, in preparation)

References

Baldwin J.A., Stone R.P.S., 1984, MNRAS, 206, 241
Becker R.H., Gregg M.D., Hook I., et al., 1997, ApJ 479, L93
Boroson T.A., Meyers K.A., 1992, ApJ 397,442
Brotherton, M.S., Tran, H.D., Van Breugel, W., Dey, A., Antonucci, R., 1997, ApJL 487, L113
Cohen, M.H., Ogle, P.M., Tran, H.D., Vermeulen, R.C., Miller, J.S., Goodrich, R.W., Martel, A.R., 1995, ApJ 448, L77
Cowie L.L., Songaila A., Egami E., et al., 1994, ApJ 432, L83.
di Serego Alighieri S., Cimatti A., Fosbury R.A.E., 1994, ApJ 431, 123
di Serego Alighieri S., 1998, in Instrumentation for Large Telescopes, Eds. J.M. Rodriguez Espinosa, Cambridge University Press, 287
Egami, E., Iwamuro, F., Maihara, T., Oya, S., Cowie, L.L., 1996, AJ 112, 73
Glenn, J., Schmidt, G.D., Foltz, C.B., 1994, ApJ 434, L47
Goodrich R.W., Miller J.S., 1995, ApJ 448, L73
Hazard C., Mc Mahon R.G., Webb J.K., Morton D.C., 1987, ApJ 323, 263
Hines, D.C., Wills, B., 1995, ApJ 448, L69
Hutsemékers, D., Lamy, H., Remy, M., 1998, A&A 340, 371
Kartje J.F., 1995, ApJ 452, 565
Lamy, H., Hutsemékers, D., 2000, A&AS, in press
Lee H.W., Blandford R.D., Western L., 1994, MNRAS 267, 303
Melnick J., Dekker H., D'odorico S., 1989, EFOSC, ESO operating manual n4, Version 2, ESO
Murray N., Chiang J., Grossman S.A., Voit G.M., 1995, ApJ 451, 498
Norman C.A., Bowen D.V., Heckman T., Blades C., Danly L., 1996, ApJ 472, 73
Ogle P.M., 1997, in ASP Conf. Ser. 128, Mass ejection from AGN, ed. N. Arav, I. Shlosman, R.J. Weymann (San Francisco:ASP), 78
Schmidt G.D., Hines D.C., 1999, ApJ 512, 125
Serkowski K., Matthewson D.S., Ford V.L., 1975, ApJ 196, 261

Sprayberry, D., Foltz, C.B., 1992, ApJ 390, 39
Stocke J.T., Morris S.L., Weymann R.J., Foltz C.B., 1992, ApJ 396, 487
Stockman H.S., Moore R.L., Angel J.R.P., 1984, ApJ 279, 485
Stone R.P.S., Baldwin J.A., 1983, MNRAS 204, 347
Wampler, E.J., Chugai, N.N., Petitjean, P., 1995, ApJ 443, 586
Weymann R.J., Morris S.L., Foltz C.B., Hewett P.C., 1991, ApJ 373, 23
Wills B.J., Netzer H., Wills D., 1985, ApJ 288, 94